Journal of Alloys and Compounds 747 (2018) 471–483

Contents lists available at ScienceDirect

Journal of Alloys and Compounds

journal homepage: http://www.elsevier.com/locate/jalcom

Structures and tensile properties of Sc-containing 1445 Al-Li alloy sheet

Zhuo-wei Peng [a], Jin-feng Li [a, *], Feng-jian Sang [a], Yong-lai Chen [b], Xu-hu Zhang [b], Zi-qiao Zheng [a], Qing-lin Pan [a]

[a] *School of Materials Science and Engineering, Central South University, Changsha 410083, China*
[b] *Aerospace Research Institute of Materials and Processing Technology, Beijing 100076, China*

ARTICLE INFO

Article history:
Received 4 November 2017
Received in revised form
3 February 2018
Accepted 4 March 2018
Available online 6 March 2018

Keywords:
Al-Li alloy
Grain structure
Non-recrystallization
Strength
Precipitates

ABSTRACT

The strength and precipitates after T8-aging (second-step aging at 170 °C following first-step aging at 150 °C for 4 h after 6% predeformation) and grain structures of 1445 Al-Li alloy (Al-1.7Li-1.5Cu-0.9Mg-0.1Mn-0.1Zr-0.1Ag-0.1Ti-0.08Sc-0.07Ni) cold-rolled sheet were investigated. The main precipitates are δ′ (Al_3Li) and S′ (Al_2CuMg). It is critical that nano-sized $Al_3(Sc,Zr)$ dispersoids are formed, and the Cu-enriched and Sc-containing W phases (AlCuSc) are not found. Due to the strong pinning effect of the nano-sized $Al_3(Sc,Zr)$ dispersoids on sub-grain boundaries and dislocations, the solutionized 1445 Al-Li alloy sheet displays non-recrystallization characteristics, which corresponds to a high volume fraction of deformation textures of Copper {112}<111>, Brass {011}<211> and S {123}<634>. This non-recrystallization feature makes the 1445 Al-Li alloy suitable for thin sheet. In addition, due to the addition of minor Ni, Al_9FeNi particles instead of Al_7Cu_2Fe particles are formed.

1. Introduction

To improve some performance characteristics including weight reduction, fuel economy, loadlifting capacity, Al-Li alloys are considered as prospective structural materials for aircraft and aerospace engineering, due to their unique combination of properties such as low density, high elastic modulus and rather high specific strength [1]. Up to now, three generations of Al-Li alloys have been developed. Among them, the third generation Al-Li alloys, including 2195, 2050, 2099, 2198, 2199 et al., have been successfully applied in launch vehicles and aircrafts [1–3].

An important composition feature of the third generation Al-Li alloys is the addition of micro-alloying elements, such as Zr, Mn, Mg, Ag and Zn. It was reported that minor Zr and Mn were added for recrystallization controllment [4,5]. The addition of Mg, Ag and Zn played an important role in improving the distribution of T1 (Al_2CuLi) precipitates. Among them, Ag or Zn element is usually added with the combination of Mg element. For example, the combination of Mg + Ag is added to 2195, 2050 and 2198 Al-Li alloys, which accelerates the aging response, increases T1 nucleation density and therefore enhances the strength [4–8]. Mg + Zn combination is added to 2099, 2199 and 2A97 Al-Li alloys, which plays a role similar to Mg + Ag combination [9,10]. In addition, minor Zn addition is found to enhance the corrosion resistance of Al-Li alloys [11,12].

Due to the formation of Al_3Sc dispersoids during solidification, thermo-mechanical process and aging at 250–350 °C, the small Sc addition (usually lower than 0.15%) in pure Al and Al-Mg alloys can obviously refine the cast grain structures, significantly inhibit recrystallization and therefore effectively strengthen the corresponding alloys by Al_3Sc precipitate strengthening, sub-structure strengthening and fine grain strengthening [13]. Sc element is also added in some Al-Li alloys developed by Russia, such as 1421, 1460, 1461 and 1469 Al-Li alloys [14]. In some Al-Cu-Li types of Al-Li alloys such as 2099 and 1460 alloys, the small addition of Sc effectively refined grain structures, inhibited recrystallization and displayed positive effect on the strength due to the formation of nano-sized $Al_3(Sc,Zr)$ dispersoids [15–18]. However, in Al-Cu alloys and some other Al-Cu-Li types of Al-Li alloys such as 1469 alloy, the small Sc addition was not found to effectively refine grain structures and inhibit recrystallization. On the contrary, it displayed negative effect on the strength due to the formation of coarse W phase (Al_8Cu_4Sc, $Al_{5\text{-}8}Cu_{7\text{-}4}Sc$ or $Al_{8\text{-}x}Cu_{4+x}Sc$) [19,20].

To meet the demand of future aerospace structures, new Al-Li

---

* Corresponding author.
E-mail address: lijinfeng@csu.edu.cn (J.-f. Li).

https://doi.org/10.1016/j.jallcom.2018.03.032
0925-8388/

alloys are still in development. Recently, Russia developed a new Al-Li alloy 1445, which was suitable for thin sheets [21]. In addition to the alloying elements of Li, Cu, Mg and Zr, a small amount of Sc is added. Meanwhile, it contains a trace amount of Ni elements, which is different from most Al-Li alloys. This case is to characterize the tensile properties and aging precipitates of this new 1445 Al-Li alloy sheet. In addition, due to the different effect (positive or negative) of the Sc addition in different Al-Li alloys, it is critical to specify the Sc micro-alloying effect in the 1445 Al-Li alloy. Another objective is to declare the existence forms of Sc and Ni elements in the 1445 Al-Li alloy.

2. Experimental

2.1. Materials and procedures

The chemical compositions of the experimental 1445 Al-Li alloy sheet are shown in Table 1. The alloy ingot was homogenized at 470 °C for 8 h followed by at 520 °C for 24 h. After homogenization, the ingots were rolled into plate with 5.6 mm thickness through hot rolling. After annealing, the plate was then cold-rolled to sheet with a thickness of 2.6 mm.

After solutionization in a salt bath furnace at 525 °C for 1 h [21] followed by quenching in water, the sheet was then subjected to a two-step T8 temper (second-step aging at 170 °C following first-step aging at 150 °C for 4 h after 6% pre-deformation through cold rolling).

2.2. Tensile tests

Tensile samples with a parallel section gauged 30 mm in length and 8 mm in width were cut from the sheet. Yield strength, tensile strength and elongation of the samples were characterized by using the MTS 858 universal testing machine with a strain rate of 1.0×10^{-3}/s at ambient temperature. Three tensile tests were performed for each condition, average strength and elongation were then calculated.

2.3. Structure observations

The metallograhical structures of the rolled and solutionized sheets were observed on the longitudinal section. The samples were mechanically ground and polished, washed ultrasonically with ethanol, and then anodically treated at 24 V in a solution containing 1.1 g H_3BO_3, 95 mL H_2O and 3 mL HF. The metallographical observations were performed through an optical microscopy (OM, Leica DMI300 M).

Particles in the cold-rolled and solutionized alloy were observed through an FEI Quanta 650 FEG scanning electron microscope (SEM) in backscattered electron (BSE) mode, and their constituent elements were analyzed through energy dispersive X-ray spectroscopy (EDS) equipped in the SEM. Element mappings of the solutionized alloy sheet were mainly determined through electron probe microanalysis (EPMA) (JXA-8800 R, JEOL, Japan) equipped with an OXFORD INCA 500 wave dispersive X-ray spectrometer (WDS).

The texture of the solutionized alloy sheet was measured through Brucker D8 Discovery X-ray diffractometer. Incomplete polar figures of {111}, {200} and {220} were detected, then the orientation distributing function (ODF) was calculated, and particle swarm optimization (PSO) was used for the quantitative analysis of the texture.

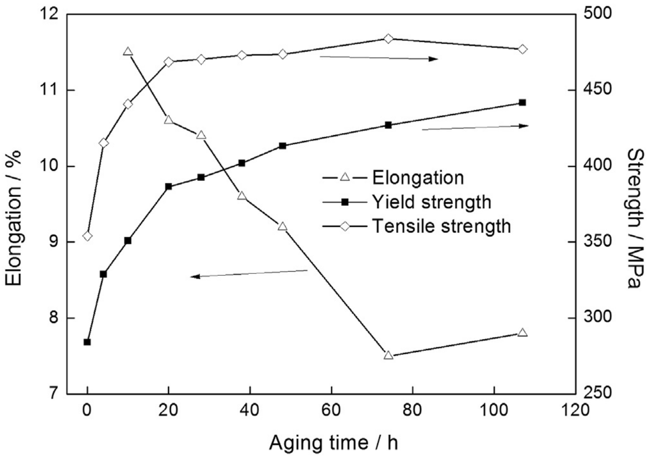

Fig. 1. Tensile property of the 1445 Al-Li alloy sheet as a function of the second-step aging time.

The grain structure and the recrystallization degree of the solutionized sheet were also observed by electron backscatter diffraction (EBSD) with a scanning step size of 0.7 μm. The EBSD data was performed using a Sirion 200 Field Emission Gun Scanning Electron Microscope (FESEM) equipped with an integrated EBSD system at an accelerating voltage of 25 kV. The OIM Analysis 5.31 software was utilized to analyze the received EBSD data. During the data analysis, a cleanup with grain tolerance of 2° was applied to re-index the data points, and two kinds of boundaries were defined. Low-angle boundary (LAB) was defined at misorientation (θ) in the range of 2°–10° ($2° < \theta < 10°$), while high-angle bounary (HAB) was defined as $\theta > 10°$.

Transmission electron microscope (TEM) was used to observe the precipitates in the aged alloy. The TEM samples were prepared by mechanical grinding and twin-jet electropolishing in a solution containing 30% nitric acid and 70% methanol (volume fraction) at −25 °C with a voltage of 15–20 V. TEM observation were carried out with a Tecnai $G^2$20 TEM operating at 200 kV through conventional dark-field (DF) imaging and selected area electron diffraction (SAED). Some observations were performed on a scanning transmission electron microscopy (STEM, Titan G^2 60–300, FEI) with spherical aberration correction, which is equipped with EDS (GENE SIS60E) and high angle annular dark field (HAADF) imaging. The STEM observation was operated at 300 kV.

3. Results

3.1. Tensile properties and precipitates of 1445 Al-Li alloy

Fig. 1 shows the tensile property of the 1445 Al-Li alloy sheet as a function of the second-step aging time. After the second-step aging for 24 h at 170 °C, the alloy reaches near peak tensile strength of about 470 MPa. Afterwards, the tensile strength keeps stable, but the yield strength still increases to 450 MPa by about 50 MPa with

Table 1
Chemical compositions of the studied 1445 Al-Li alloy sheet (mass fraction, %).

Cu	Li	Mg	Ag	Mn	Sc	Zr	Ni	Ti	Al
1.5	1.7	0.9	0.1	0.1	0.08	0.1	0.07	0.1	Bal.